ARTICLE

JAAS www.rsc.org/jaas

Aerosol diagnostics and inductively coupled plasma mass spectrometry with demountable concentric nebulizers

Su-Ann E. O'Brien Murdock,[a] Kaveh Kahen,[a] José R. Chirinos,[a]† Michael E. Ketterer,[b] David D. Hudson[b] and Akbar Montaser*[a]

[a]*Department of Chemistry, The George Washington University, Washington DC 20052, USA. E-mail: montaser@gwu.edu; Fax: 202-994-2298; Tel: 202-994-6480*

[b]*Department of Chemistry, Northern Arizona University, Box 5698, Flagstaff AZ 86011, USA*

Received 14th August 2003, Accepted 16th January 2004
First published as an Advance Article on the web 7th April 2004

A demountable concentric nebulizer (DCN) is evaluated for inductively coupled plasma mass spectrometry (ICPMS). This nebulizer operates at conditions similar to a commercial pneumatic nebulizer used in ICP spectrometries, but is easily fabricated and is considerably less expensive. Key aerosol diagnostics data, and analytical figures of merit are presented for the DCN used in ICPMS. The DCN produces a better quality primary aerosol when using inner capillaries of smaller diameters. At a solution uptake rate of about 500 μL min^{-1} and a nebulizer gas flow rate of 1.0 L min^{-1}, the Sauter mean diameter ($D_{3,2}$) of the primary aerosol of the DCN is 7 μm and 14 μm for solution capillaries having an i.d. of 95 μm (DCN-1) and 190 μm (DCN-2), respectively. Based on the cumulative mass percent data, nearly 70% of the total mass of the droplets produced by DCN-1, under the above conditions, is composed of droplets having sizes less than 10 μm. The $D_{3,2}$ of the tertiary aerosol of DCN-1, under the same operating conditions, is reduced to 5 and 3 μm when the nebulizer is coupled to a Scott-type and a cyclonic spray chamber, respectively. The tertiary aerosol of the DCNs studied does not show substantially different $D_{3,2}$ values, particularly when the cyclonic spray chamber is used. Under optimum conditions, detection limits, sensitivities, and precision for the DCN compare favorably with a commercially available crossflow nebulizer. The accuracy and precision of the DCN in ICPMS measurements are demonstrated using two standard reference materials: SRM 1643c (Trace Elements in Water), and SRM 1570 (Trace Elements in Spinach).

Introduction

The most common form of sample in inductively coupled plasma (ICP) spectrometry is the liquid form.[1,2] Many devices have been developed and are in use for aerosol generation and transport, each however, with its own benefits and limitations.[3,4] The typical pneumatic nebulizer spray chamber arrangement is simple and inexpensive, however, it suffers from the drawbacks of large sample consumption (1–2 mL min^{-1}), low analyte transport efficiency (1–20%), and memory effects. Several microflow nebulizer spray chamber arrangements have been investigated to reduce sample consumption and enhance analyte transport efficiency.[3] The major devices include the high efficiency nebulizer (HEN),[5–10] the microconcentric nebulizer (MCN),[11,12] and the Micromist.[13] Two major micronebulizers are used to introduce 100% of the sample into the plasma, without a spray chamber, and with minimal memory effects: the direct injection nebulizer (DIN),[14–17] and the direct injection high efficiency nebulizer (DIHEN).[13,18–26] These devices are well suited for applications involving expensive, toxic, or limited volume samples. In general, both the DIN and the DIHEN offer similar or better sensitivity, precision, and detection limits than the conventional nebulizer spray chamber combination. One drawback of the micronebulizers is the susceptibility to greater nebulizer clogging compared to the conventional devices, as well as higher cost.

In this study, a demountable concentric nebulizer (DCN) is described that can be easily constructed from fused silica tubing and surgical pipettes at a very low cost. The DCN is generally similar to earlier devices[27,28] in that the solution capillary is easily adjusted for optimization, or replaced in the event of nebulizer clogging. Unfortunately, little[28] or no[27] information has been published on the analytical performance and aerosol characteristics of the cited devices. In this report, we present key aerosol diagnostics data and analytical figures of merit for the DCN as used in ICP-MS. Further, the analytical utility of the DCN is investigated using two standard reference materials: SRM 1643c (Trace Elements in Water), and SRM 1570 (Trace Elements in Spinach).

Experimental

The demountable concentric nebulizer

Table 1 presents the critical dimensions of two DCNs tested in this work, along with the same data for two commercial nebulizers: a HEN and a conventional nebulizer (Meinhard Glass Products, a division of Analytical Reference Materials International Corp., Golden, CO). The 13 major components of the DCN are shown in a schematic (Fig. 1). Both the inner and outer capillaries, and the brass components, are commercially available and easily replaceable. Component 1 is a 15 cm long solution capillary which does not taper and is made of a polyimide coated, non-deactivated, fused-silica tubing (Alltech, Deerfield, IL), having internal diameters of 95 (DCN-1) or 190 μm (DCN-2). Component 2 is an 8-cm long 100 μL surgical pipette (Corning, Acton, MA) that serves as the gas nozzle. The gas nozzle is sheathed with component 3, a ¼ inch polyethylene tubing (Swagelok, Solon, OH), to securely fit the DCN assembly to a standard spray chamber. Component 4 is a brass tee (Swagelok), having three ¼ inch brass nuts marked as component 5, for connection to the nebulizer gas inlet (using component 6, a ¼ inch nylon tubing and component 7, a ¼

† On leave from Centro de Química Analítica, Universidad Central de Venezuela, Caracas 1041a, Venezuela.

DOI: 10.1039/b309670g

Table 1 Critical dimensions for the demountable concentric nebulizers[a]

Nebulizer type	DCN-1	DCN-2	HEN[b](HEN-170-AA)	Conventional nebulizer[b] (TR-30-AA)
Solution capillary i.d./μm	95	190	70–110	220–320
Capillary wall thickness/μm	50	60	15–40	15–40
Gas orifice i.d./μm	285	390	150–200	350–450
Capillary annulus area/mm^2	0.0071	0.0283	0.0038–0.0095	0.05–0.10
Gas annulus area/mm^2	0.032	0.046	0.007–0.01	0.03–0.04

[a] All dimensions were measured using a trinocular microscope (Model ZST ZOOM, Unitron Inc., Bohemia, NY). [b] Values provided courtesy of Meinhard Glass Products, a division of Analytical Reference Materials International Corp.

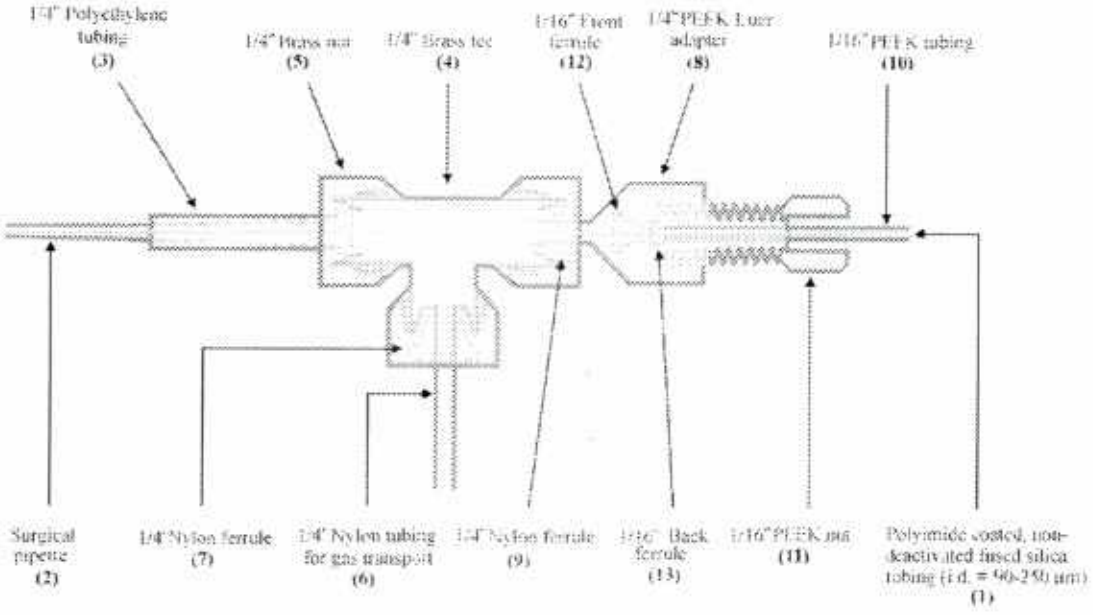

Fig. 1 Schematic diagram of the demountable concentric nebulizer (DCN)

inch nylon ferrule, both from Swagelok), the polyethylene tubing (component 3), and the solution delivery inlet (using a ¼ inch PEEK Luer adapter from Alltech Associates Inc., marked as component 8, which fits snuggly into the brass nut, and a ¼ inch nylon ferrule from Swagelok shown as component 9, which serves to hold component 8 in place). For solution delivery, the inner capillary is sheathed with component 10, 5 cm of a 508 μm id PEEK tubing (Upchurch Scientific), through component 11, a 1/16 inch PEEK nut (Upchurch Scientific) to form a gas tight seal to the PEEK Luer adapter (component 8) using 1/16 inch front and back ferrules (components 12 and 13) from Upchurch Scientific.

The injector gas flow rate ranges from 0.4 to 1.4 L min^{-1} and is controlled by an external mass flow-controller (Model 8200, Matheson Gas Products, Montgomeryville, PA). Solution is delivered to the nebulizer in a continuous flow mode with a four channel peristaltic pump (Model Rabbit, Rainin Instrument Co., Inc., Woburn, MA) at the rate of 0.085 to 1 mL min^{-1}. Narrow-bore tygon tubings (0.015 and 0.030 in i.d., Astoria-Pacific Inc., Clackamas, OR) are utilized to reduce peristaltic related noise.

Aerosol diagnostic by phase Doppler particle analysis

Aerosol diagnostics were conducted with the two DCNs. The droplet size and velocity distributions of the aerosols were simultaneously determined using a two-dimensional phase Doppler particle analyzer (2D-PDPA, Aerometrics/TSI Inc., St Paul, MN). The PDPA system is described elsewhere.[18] The DCN was positioned horizontally, as it is used in ICPMS, for sampling the aerosol. The receiver optics were held at a forward scattering angle of 30° with respect to the transmitter by placing both the receiver and the transmitter on 15° inclined planes to allow horizontal aerosol sampling. The four photomultiplier tubes were operated at −501 V. The width of the probe volume was ~120 μm, using a 250 mm focal length transmitting lens and a beam separation of 41 mm. By comparing the spatial phase difference measured across three detectors, the scattering from non-spherical droplets or multiple droplets in the sampling volume were rejected. Phase shift differences (between different pairs of detectors) exceeding 6% were discarded. In general, less than 5% of the sampled droplets were discarded.

The primary aerosol was sampled 15 mm from the nebulizer tip along the centerline of the aerosol. The tertiary aerosol was sampled 10 mm from the end of the spray chamber, and at the centerline of the chamber exit. In each case, the droplet size and velocity distributions were determined by sampling approximately 10,000 droplets. Velocities were measured axially along the centerline of the spray and radially with the velocity component perpendicular to the centerline. The droplet size distribution was expressed in terms of Sauter mean diameter ($D_{3,2}$), which is defined as the volume-to-surface area ratio of the aerosol. An average of three measurements (30,000 droplets) was used to obtain $D_{3,2}$ and mean velocity values. The precision of the $D_{3,2}$ and mean velocity values ranged from 0.5 to 2% RSD for 3 consecutive measurements on the same DCN. Higher %RSD values (up to 10–15%) in $D_{3,2}$ were observed due to variation in aerosol probing position from one day to another, particularly when the DCN was disassembled and reassembled.

Table 2 Operating conditions for the Ar ICP-MS instrument[a]

ICPMS system	PE-Sciex Elan 6000
RF power/W	1400
Nominal frequency/MHz	40
RF generator type	Free-running
Induction coil circuitry	3-turn copper coil, PlasmaLock®
Sampling depth (above load coil)/mm	11
Sampler (orifice diameter/mm)	Nickel, (1.1)
Skimmer (orifice diameter/mm)	Nickel, (0.9)
Outer gas flow rate/L min^{-1}	15
Intermediate gas flow rate/L min^{-1}	1.2
Solution flow mode	Continuous
Spray chamber	Scott-type (100 mL), Cyclonic-type (20 mL)
Data acquisition parameter	
Scan mode	Peak hopping
Points/Mass	1
Resolution/amu	0.7
Sweeps per reading	10
Readings per replicates	5
Replicates	11
Dwell time per mass/ms	20
Integration time/s	1

[a] Unless otherwise indicated.

The ICPMS instrument

An Elan 6000 ICPMS system (PerkinElmer/Sciex Corporation, Norwalk, CT) was used to investigate analytical characteristics of the nebulizer under the conditions listed in Table 2. The ICPMS figures of merit were obtained for DCN-1 having a solution capillary id of 95 μm, using two spray chambers: a Scott-type (PerkinElmer/Sciex Corporation) and a cyclonic-type (LECO Corporation, St. Josephs, MI). This solution capillary has dimensions similar to those used for the HEN[7] and the DIHEN.[18] All analytical data were obtained under standard laboratory conditions (*e.g.* not in a clean-room environment). The maximum ion intensity of $^{103}Rh^+$ was used for daily optimization. The system was set to peak-hopping mode with a dwell time of 20 ms and total integration time of 1 s mass^{-1}. The lens voltage was auto-optimized daily for each *m/z*.

Reagents and sample preparation

Distilled deionized water (DDW, 18.3 MΩ cm) was used for collection of the aerosol diagnostics data. For ICP-MS measurements, a 10 ng mL^{-1} multi-element standard solution was prepared by diluting 1000 μg mL^{-1} stock solution (Spex Certiprep Inc., Metuchen, NJ) with 2% high-purity HNO_3 (Optima grade, Fisher Scientific, Pittsburgh, PA) in DDW. Technique validation was accomplished using Trace Elements in Water (SRM 1643e) and Trace Elements in Spinach (SRM 1570) obtained from the National Institute of Standards and Technology (NIST), Gaithersburg, MD. The spinach sample (0.3 g) was dissolved in 7 mL of HNO_3 (70% v/v) using a closed vessel microwave digestion system (Model MDS 2000, CEM Corporation, Mathews, NC). The digestion program involved a 10 min, five-stage heating cycle at 40, 85, 135, 150, and 180 psi., with a 5 min ramp time in between each stage. After cooling, the digested sample was transferred to a 250 mL flask and diluted with deionized water. A four-point standard addition curve was used to quantify the elements.

Results and discussion

The extent of the desolvation–vaporization–atomization processes in the plasma depends greatly on the size and velocity of the sample droplets introduced. Furthermore, suppression of vaporization and ionization is likely to occur near large droplets and significant fluctuation of analyte emission and ionization can occur near desolvating and vaporizing droplets.[29–31] For ICP spectrometry, the ideal aerosol should consist of small monodispersed droplets with uniform velocity.[32,33] Deviations from the cited criteria cause precision, sensitivity and detection limits to suffer. In this connection, we examined the characteristics of the primary and tertiary aerosol produced by DCNs having different solution capillary diameters.

Droplet size and velocity distributions — primary aerosol

Representative primary droplet size distributions are presented in Figs. 2 and 3 for the DCNs. The nebulizers are operated at a nebulizer gas flow rate and solution uptake rate of 1.0 L min^{-1} and 510 μL min^{-1}, respectively. A decrease in the id of the solution capillary results in reduced droplet diameter (Fig. 2A), similar to the trend earlier established for the HEN compared to the conventional concentric nebulizer.[7,33–36] For example, with a 190 μm i.d. capillary, $D_{3,2}$ is 14 μm, double the value (7 μm) obtained with a solution capillary i.d. of 95 μm. Normalized volume distributions (Fig. 2B) also reveal that larger droplets are produced with the 190 μm i.d. solution

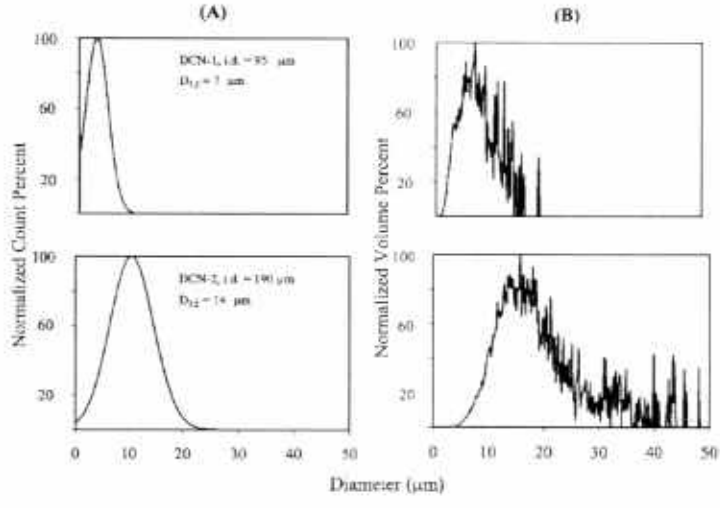

Fig. 2 Primary droplet size distribution in (A) normalized count percent and in (B) normalized volume percent for DCN-1 and DCN-2 with solution capillaries having diameters of 95 and 190 μm, respectively. Each distribution represents approximately 10,000 droplets. The water aerosol produced at a solution flow rate of 510 μL min^{-1} was probed at 15 mm from the tip of the DCN along the centerline of the aerosol cone. The nebulizer gas flow rate was 1.0 L min^{-1}.

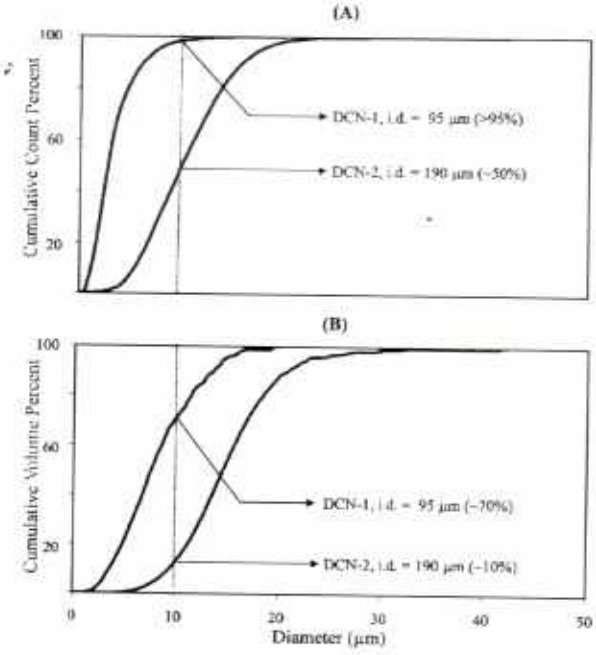

Fig. 3 Plots of (A) cumulative count and (B) volume percent as a function of primary droplet diameter for DCN-1 and DCN-2 with solution capillaries having diameters of 95 and 190 μm, respectively. Each distribution represents approximately 10,000 droplets. The water aerosol produced at a solution flow rate of 510 μL min^{-1} was probed at 15 mm from the tip of the nebulizer along the centerline of the aerosol cone. The nebulizer gas flow rate was 1.0 L min^{-1}.

capillary. The largest droplet produced by DCN-1 and DCN-2 is approximately 20 μm and 50 μm, respectively (Fig. 2B).

Based on the cumulative count percent data (Fig. 3A), approximately 50% of the droplets are below 10 μm for the primary aerosol of the DCN having a 190 μm i.d. solution capillary. Over 95% of the droplets produced by the DCN having a 95 μm i.d. capillary are below 10 μm. In general, droplets below 8–10 μm in diameter are more easily desolvated–vaporized–atomized in the ICP and contribute favorably to the signal intensity.[29] However, it is cumulative volume (or mass) percent (Fig. 3B), which correlates well with the analytical signal. Nearly 70% of the total mass of the droplets produced by the DCN having a solution capillary i.d. of 95 μm is composed of droplets having sizes less than 10 μm. This value for the DCN having the 190 μm i.d. capillary is 10%. In summary, among the two DCNs tested, DCN-1 produces the smaller droplets.[33–37]

Figs. 4 to 6 show primary droplet size and velocity distributions for DCN-1 (95 μm i.d. capillary) as a function of nebulizer gas flow rate, ranging from 0.4 to 1.0 L min^{-1}. A greater number of large droplets are produced at low nebulizer gas flow rates (Fig. 4A and Fig. 5A). For example, at 0.4 L min^{-1}, $D_{3,2}$ is 15 μm, approximately two times greater than droplets produced at 1.0 L min^{-1} (7 μm). The normalized size distributions (volume percent shown in Fig. 4B) reveal that the larger droplets (above 10 μm) produced at lower gas flow rate constitute a significant part of the sample aerosol. As illustrated in Fig. 5B, only 20% of the aerosol mass is composed of droplets less than 10 μm, at a nebulizer gas flow rate of 0.4 L min^{-1}. For a nebulizer gas flow rate of 1.0 L min^{-1}, approximately 70% of the aerosol mass produced by the nebulizer is below 10 μm.

Fig. 6 shows axial and radial droplet velocity distributions for the primary aerosol. With increasing nebulizer gas flow rate, both the axial and radial velocities become broader, with the axial mean velocity increasing significantly. For example, the mean axial velocity (and the radial root mean square velocity) at 0.4 and 1.0 L min^{-1} is 12 m s^{-1} (1.8 m s^{-1}) and 43 m s^{-1} (3.1 m s^{-1}), respectively. The lower mean droplet

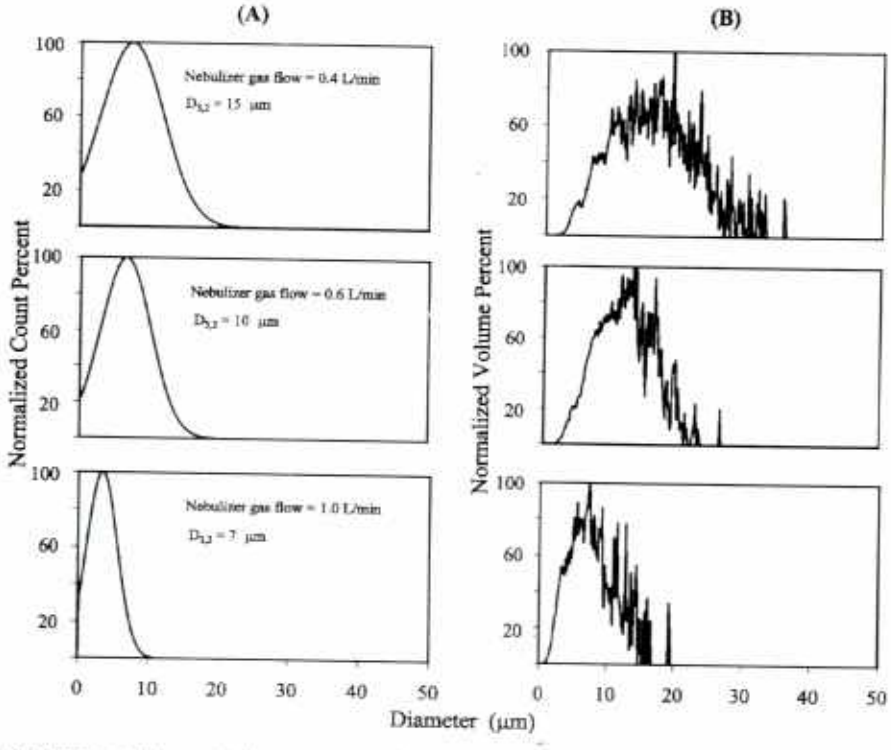

Fig. 4 Droplet size distribution in (A) normalized count percent and in (B) normalized volume percent as a function of nebulizer gas flow rate for DCN-1 (solution capillary i.d. = 95 μm). Each distribution represents approximately 10,000 droplets. The water aerosol produced at a solution flow rate of 510 μL min^{-1} was probed at 15 mm from the tip of the nebulizer along the centerline of the aerosol cone.

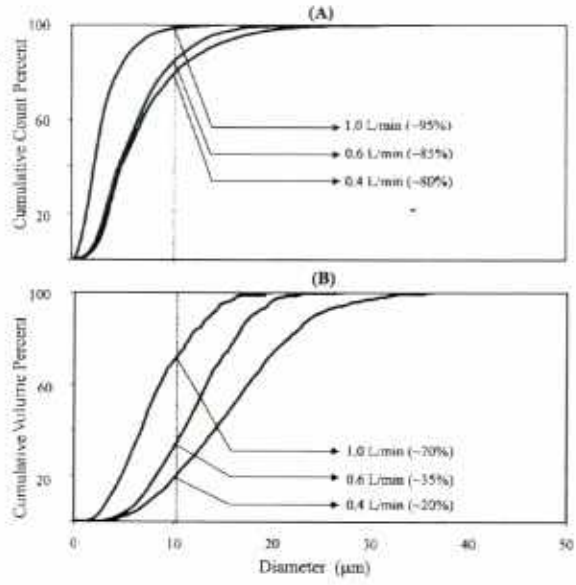

Fig. 5 Plots of (A) cumulative count and (B) volume percent as a function of primary droplet diameter at several nebulizer gas flow rates for the DCN-1 (solution capillary i.d. = 95 μm). Each distribution represents approximately 10,000 droplets. The water aerosol produced at a solution flow rate of 510 μL min^{-1} was probed 15 mm from the tip of the nebulizer along the centerline of the aerosol cone.

velocities obtained at 0.4 L min^{-1} provide longer residence time in the plasma for better desolvation, vaporization, and atomization of the large droplets, particularly because the number of droplets having the most probable velocity is large. Note that the radial velocity profile does not exhibit a symmetric distribution indicating that the aerosol cone is not symmetrically distributed for the DCN tested. This asymmetry, as shown later under analytical figures of merit, results in reduced sensitivity and higher detection limits when a small-sized spray chamber, such as the cyclonic spray chamber, is used. The interaction of the aerosol cone with one side of the cyclonic spray chamber surface apparently reduces analyte transport efficiency, leading to inferior analytical figures of merit. We speculate that the asymmetry of the aerosol cone is due to the greater imperfections of the surgical pipette tip compared to the gas nozzles used in the commercial nebulizers, and to the lack of an adequate tangential gas flow to center the solution capillary in the gas nozzle. The latter is attributed to the large void volume of several components such as the brass tee (component 4), the surgical pipette (component 2), and the fused silica tubing (component 1) not being tapered.

Droplet size and velocity distribution—tertiary aerosol

Representative tertiary droplet size distributions are presented in Fig. 7 for DCN-1 (solution capillary, 95 μm i.d.) and DCN-2 (solution capillary, 190 μm i.d.) using Scott-type and cyclonic spray chambers. Both spray chambers reduce the droplet size distribution to less than 10 μm. For example, $D_{3,2}$ for the primary aerosol of DCN-2 is 14 μm. This is reduced to 7 μm and 4 μm, using a Scott-type and cyclonic spray chamber, respectively. In effect, the spray chambers are acting as a filter with a fixed cut off droplet diameter.[33,36] This reduction in size is in agreement with previous studies using a HEN and a Scott-type spray chamber.[7] The cyclonic spray chamber is more effective in eliminating large droplets, thereby exhibiting a narrower droplet size distribution, compared to the Scott-type. This finding is not in agreement with previous work, perhaps due to the asymmetry of the aerosol cone of the DCN. For instance, despite the large difference between the primary aerosol of DCN-2 ($D_{3,2}$ = 14 μm) and DCN-1 ($D_{3,2}$ = 7 μm),

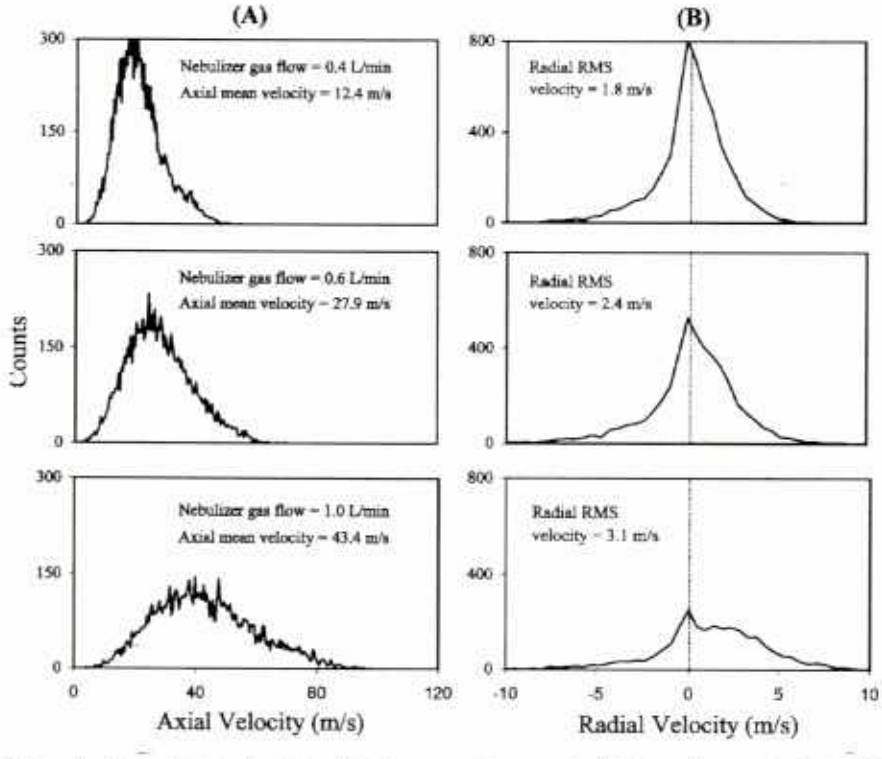

Fig. 6 Variation of (A) axial and (B) radial droplet velocity distributions as a function of nebulizer gas flow rate for the DCN-1 (solution capillary i.d. = 95 μm). Each distribution represents approximately 10,000 droplets. The water aerosol produced at a solution flow rate of 510 μL min^{-1} was probed at 15 mm from the tip of the nebulizer along the centerline of the aerosol cone.

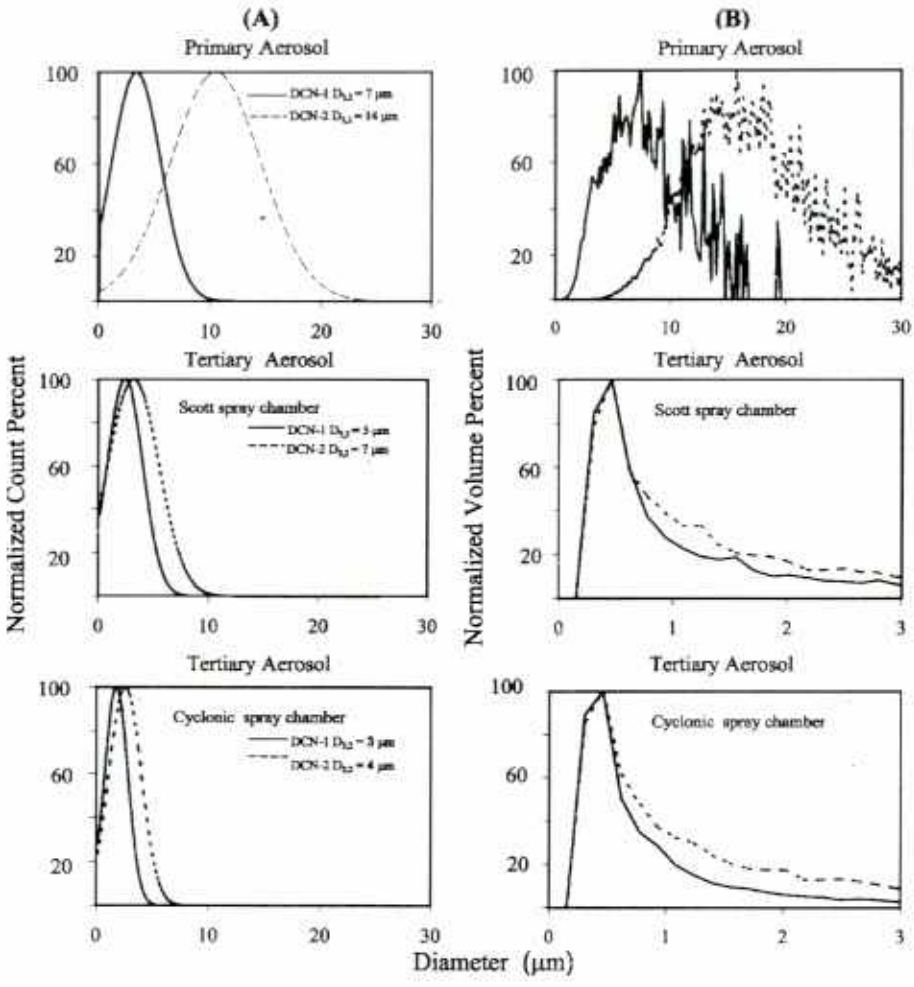

Fig. 7 Primary and tertiary droplet size distribution in (A) normalized count percent and in (B) normalized volume percent for DCN-1 and DCN-2 at a nebulizer gas flow rate of 1.0 L min^{-1}. Each distribution represents approximately 10,000 droplets. The primary aerosol produced at a solution flow rate of 510 μL min^{-1} was probed at 15 mm from the tip of the nebulizer along the centerline of the aerosol cone. The tertiary aerosol was probed at 10 mm from the centerline of the spray chamber.

the tertiary aerosol is extremely fine, having $D_{3,2}$ values of 4 μm and 3 μm, respectively, when the cyclonic spray chamber is used.

Operating conditions for the DCN using ICP-MS

Among the DCNs tested, DCN-1 (solution capillary, 95 μm id) provides a finer primary aerosol, and thus it was selected for ICPMS studies. The effects of nebulizer gas flow rate, RF power, and solution uptake rate on signal intensity are shown in Fig. 8 for several elements across the mass range. These results are obtained using a Scott-type spray chamber. The maximum sensitivity for the elements tested is found at a nebulizer gas flow rate of 1.0 L min^{-1} (Fig. 8A), similar to conventional nebulizers.[38–40] High RF powers are required for optimal sensitivity (Fig. 8B), with the optimum being at 1400 W. The signal intensities of the test elements increase only by a factor ranging from 1.5 to 2 as the solution uptake rate is changed from 100 μL min^{-1} to 650 μL min^{-1}, with no significant improvement beyond this level (Fig. 8C). Similar nebulizer gas flow rate and RF power are found for the same nebulizer using a cyclonic spray chamber; however, the optimum solution uptake rate is 950 μL min^{-1}.

Oxides and doubly charged species

The level of oxides and doubly charged species in ICP-MS are of concern because they contribute to serious spectral interferences.[1,41,42] For conventional nebulizers, both the MO^+/M^+ and M^{++}/M^+ ratios are strong functions of the nebulizer gas flow rate and the solvent load. Oxide ratios can be reduced by lowering the nebulizer gas flow rate, using mixed-gas plasmas or applying aerosol desolvation.[43–46] Fig. 9A shows the intensities of Ce^+, CeO^+ and CeO^+/Ce^+ as a function of nebulizer gas flow rate. The CeO^+/Ce^+ ratio significantly increases (over 100%) at nebulizer gas flow rates greater than 1.0 L min^{-1} due to the significant reduction and increase in Ce^+ and CeO^+ signal intensities, respectively. This ratio also increases with solution uptake rate (Fig. 10A) due to increased solvent load of the plasma. At optimum conditions (maximum Ce^+ intensity), the DCN produces a CeO^+/Ce^+ ratio of 9%, similar to that obtained with a conventional pneumatic nebulizer (11%).[47] The lowest CeO^+/Ce^+ ratio is obtained at a nebulizer gas flow rate of 0.6 L min^{-1} (1.3%). Under this condition, the Ce^+ intensity is reduced by a factor of 50, compared to the optimum condition for Ce^+ measurements. Thus a nebulizer gas flow rate of 1.0 L min^{-1} was used to conduct measurements.

The effect of the nebulizer gas flow rate and solution uptake

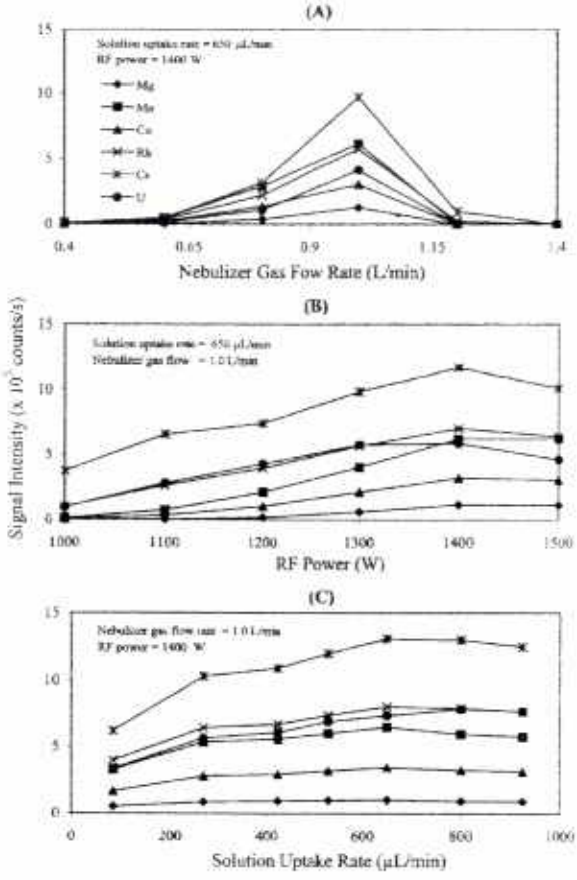

Fig. 8 Signal intensity for several elements as a function of (A) nebulizer gas flow rate, (B) RF power and (C) solution uptake rate for the DCN-1 used with Scott-type spray chamber.

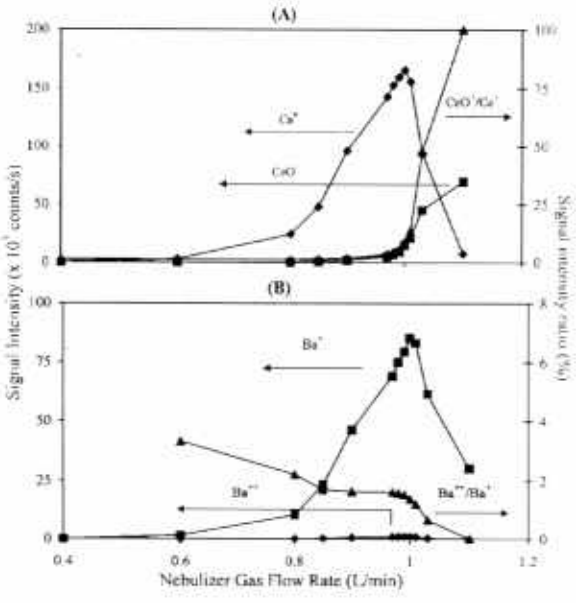

Fig. 9 Signal intensity and ion intensity ratios for oxides and doubly charged species as a function of nebulizer gas flow rate for the DCN-1 used with Scott-type spray chamber. The solution uptake rate = 650 µL min^{-1} and RF power = 1400 W.

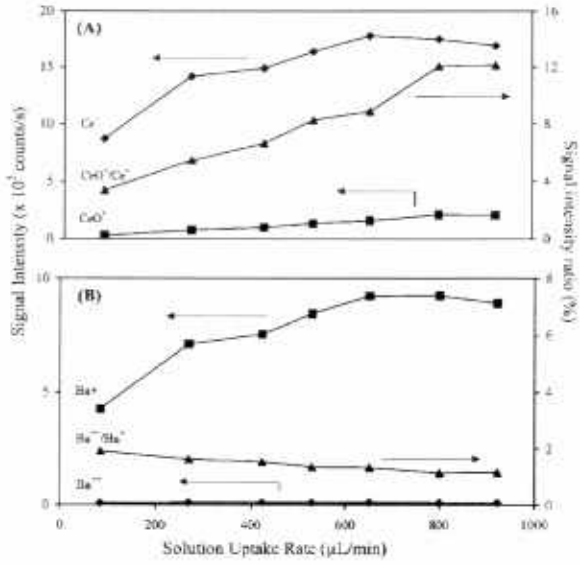

Fig. 10 Signal intensity and ion intensity ratios for oxides and doubly charged species as a function of solution uptake rate for the DCN-1 used with Scott-type spray chamber. The nebulizer gas flow rate = 1.0 L min^{-1} and RF power = 1400 W.

rate on doubly charged ions is presented in Figs. 9B and 10B, respectively, for several barium species. Note that the Ba^{++}/Ba^{+} ratio is reduced significantly at nebulizer gas flow rates above 1.0 L min^{-1} (Fig. 9B) but is almost independent of solution uptake rate (Fig. 10B), producing ratios less than 2%, under optimum conditions, again similar to data obtained with conventional pneumatic nebulizers.[48] Similar trends are observed with the same nebulizer using a cyclonic spray chamber.

Detection limits, sensitivity, and precision for DCN

Sensitivity, relative detection limits (based on 3σ of the blank signal), and short-term precision (5 min) are presented in Table 3, for several elements, for DCN-1 operated in the continuous flow nebulization mode under the optimum conditions. In general, the DCN-Scott type spray chamber arrangement provides superior detection limits, sensitivity, and precision than the DCN-cyclonic spray chamber, despite the finer aerosol obtained by the cyclonic spray chamber. This apparent discrepancy may be attributed to the asymmetry of the aerosol cone. For most elements, a factor of 2 to 5 improvement in detection limits is achieved with the Scott-type spray chamber, however greater improvements are observed for Tm, Th, and U (a factor of 10 to 30). At a solution uptake rate of 650 µL min^{-1}, the DCN-Scott type spray chamber provides similar or better detection limits compared to the crossflow nebulizer for most elements tested, by up to a factor of 3 (Table 3). Because of the smaller size of the solution capillary, the detection limits measured with the DCN in the microflow mode (85 µL min^{-1}) are generally better than those for the crossflow nebulizer by a factor of 2 to 20 (Table 4). A similar finding was noted for the HEN in comparison to the conventional nebulizer.[5] The sensitivity of the DCN is better for the lower mass elements, but worse with the higher mass elements. In general, detection limits and sensitivity obtained with the DCN are not deteriorated significantly, compared to the crossflow nebulizer, as the solution uptake rate is reduced. For example, for the DCN, a factor of 2 to 4 deterioration is observed for most elements as solution uptake rate is reduced from 650 to 85 µL min^{-1}, except for Cu (a factor of 80) due to poor precision of the blank. For

Table 3 Relative detection limits, sensitivity, and precision for the DCN-1 and crossflow nebulizer

Nebulizer		Detection limit[a] (ppt)			Sensitivity/MHz ppm^{-1}			Precision[b] (%RSD)		
		DCN		Crossflow	DCN		Crossflow	DCN		Crossflow
Spray chamber		Cyclonic	Scott-type	Scott-type	Cyclonic	Scott-type	Scott-type	Cyclonic	Scott-type	Scott-type
Solution uptake rate/μL min^{-1}		950	650	1000	950	650	1000	950	650	1000
Element	Mass									
Mg	24	28	11	24	5	10	6.4	2.0	1.2	1.1
V	51	7	4	6	19	25	19	1.8	1.1	1.4
Mn	55	9	4	5	45	59	32	2.0	0.9	1.6
Co	59	2	1	2	23	32	26	1.8	0.8	1.2
Cu	63	16	5	9	12	16	10	1.5	0.9	0.7
Sr	88	1	0.6	0.9	51	65	51	1.9	1.1	1.0
Rb	103	1	0.2	0.6	54	53	47	1.8	1.0	1.1
In	115	2	0.4	0.6	65	42	60	1.8	1.1	1.1
Cs	133	1	0.3	0.6	87	49	80	1.6	0.9	1.1
Tm	169	1	0.1	0.3	95	87	106	1.7	1.1	0.9
Pb	208	5	3	2	27	25	40	1.8	1.1	1.0
Th	232	30	1	0.6	34	24	94	1.7	0.7	0.8
U	238	1	0.1	0.3	37	41	98	1.8	1.3	0.8

[a] Based on 3σ of the blank solution, measured at the mass of the analyte. [b] Measured over 7 min, $N = 11$. Values for crossflow nebulizer taken from ref. 18.

Table 4 Relative detection limits, sensitivity, and precision for the DCN-1 and crossflow nebulizers coupled to a Scott-type spray chamber

Nebulizer		Detection limit[a] (ppt)				Sensitivity/MHz ppm^{-1}				Precision[b] (%RSD)			
		DCN		Crossflow		DCN		Crossflow		DCN		Crossflow	
Solution uptake rate/μL min^{-1}		85	650	85	1000	85	650	85	1000	85	650	85	1000
Element	Mass												
Mg	24	53	11	150	24	5	10	1.5	6.4	2	1.2	1.7	1.1
V	51	15	4	25	6	11	25	4.0	19	1.5	1.1	1.6	1.4
Mn	55	10	4	170	5	25	59	7.2	32	1.4	0.9	1.6	1.6
Co	59	3	1	39	2	12	32	5.7	26	1.5	0.8	1.3	1.2
Cu	63	401	5	320	9	7	16	2.5	10	1.7	0.9	2.0	0.7
Sr	88	2	0.6	29	0.9	29	65	12	51	1.3	1.1	1.3	1.0
Rb	103	0.4	0.2	9	0.6	24	53	11	47	1.3	1.0	0.9	1.1
In	115	0.8	0.4	6	0.6	19	42	14	60	1.6	1.1	1.0	1.1
Cs	133	0.6	0.3	5	0.6	40	89	18	80	1.2	0.9	1.0	1.1
Tm	169	0.3	0.1	4	0.3	41	95	23	106	1.5	1.1	1.3	0.9
Pb	208	10	3	20	2	11	27	8.6	40	1.3	1.1	1.2	1.0
Th	232	13	1	5	0.6	16	34	22	94	1.2	0.7	1.0	0.8
U	238	0.6	0.1	5	0.3	18	41	23	98	1.6	1.3	0.9	0.8

[a] Based on 3σ of the blank solution, measured at the mass of the analyte. [b] Measured over 7 min, $N = 11$. Values for crossflow nebulizer taken from ref. 18.

the crossflow nebulizer, detection limits deteriorate by a factor of 3 to 30 as the solution uptake rate is reduced to 85 μL min^{-1}. Analyte precision values are generally similar with both nebulizers, on the order of 1–2%.

The nebulizer reproducibility was also tested by carefully demounting and reassembling the device and then by re-evaluating figures of merit using ICPMS. In three separate sets of studies, detection limits generally do not change by more than a factor of 2.

Analysis of SRM 1643c and SRM 1570

The DCN-1 was applied to the analysis of two SRMs: SRM 1643c (Trace Elements in Water) and SRM 1570 (Trace Elements in Spinach). Five test elements (Cu, Cr, Pb, Rb and Zn) were selected. The results of analysis are listed in Table 5. Generally, the measured values are in agreement (confidence level of 95%) with the certified values, except for Zn in water. The high level of Zn may be attributed to contamination.

Table 5 Trace elements in water and spinach 'standard reference materials'[a,b]

Element	Isotope	Water (SRM 1643c)		Spinach (SRM 1570)	
		Found/ng mL^{-1}	Certified/ng mL^{-1}	Found/μg g^{-1}	Certified/μg g^{-1}
Cu	63	22.1 ± 0.6	22.3 ± 0.6	12.4 ± 0.6	12.0 ± 6
Zn	64	82 ± 3	73.9 ± 2.9	51 ± 3	50 ± 6
Rb	85	10.9 ± 0.3	11.4 ± 0.6	12.1 ± 0.3	11.8 ± 0.6
Pb	208	36.8 ± 1.3	35.3 ± 2.9	1.2 ± 0.6	1.23 ± 0.1
Cr	52	19.3 ± 1.0 –	19.0 ± 1.9	5.6 ± 0.3	4.6 ± 1.9

[a] The nebulizer gas flow rate, rf power, and solution flow rate were 1.0 L min^{-1}, 1400 W, and 650 μL min^{-1}, respectively. [b] Values reported at 95% confidence interval.

Conclusions

A low cost, easily demountable, concentric nebulizer is explored for plasma spectrometry. Droplet size analysis shows that a better quality aerosol is obtained by decreasing the internal diameter of the solution capillary. Droplet velocity measurements reveal increased asymmetry in the aerosol cone compared to commercial nebulizers. This asymmetry results in aerosol loss, and thus ICPMS sensitivity, due to impaction with the walls of small spray chambers, such as the cyclonic spray chamber, as well as lower cut-off droplet diameter leading to lower transport efficiency of the cyclonic spray chamber. Consequently, the DCN-cyclonic spray chamber arrangement provides detection limits, sensitivity, and precision that are less favorable than the DCN-Scott type spray chamber. The DCN-Scott type spray chamber arrangement provides similar or better detection limits compared to the crossflow nebulizer. Under optimum operating conditions, CeO^+/Ce^+ and Ba^{++}/Ba^+ ratios are similar to those measured for commercial pneumatic nebulizers. Analysis of two standard reference materials show that the DCN results are in general agreement with the certified values. The simplicity of the DCN described in this work facilitates changes in critical nebulizer dimensions for fundamental studies. In terms of practical use, the device is useful in that the solution capillary may be replaced in case of clogging. However, the simplicity of the DCN clearly results in some drawbacks such as formation of an asymmetrical aerosol cone compared to commercial nebulizers.

Acknowledgements

This research was sponsored by Grants from the US Department of Energy (DE-FG02-93ER14320), and the National Science Foundation (CHE-9505726 and CHE-9512441). The authors thank Billy W. Acon, John A. McLean, Michael G. Minnich and Craig S. Westphal of George Washington University for their contributions during the course of this study and in the preparation of this manuscript.

References

1 A. Montaser, *Inductively Coupled Plasma Mass Spectrometry*, Wiley-VCH, New York, 1998.
2 A. Montaser and D. W. Golightly, *Inductively Coupled Plasmas in Analytical Atomic Spectrometry*, 2nd edn., Wiley-VCH, New York, 1992.
3 A. Montaser, M. G. Minnich, J. A. McLean, H. Liu, J. A. Caruso and C. W. McLeod, in *Inductively Coupled Plasma Mass Spectrometry*, ed. A. Montaser, Wiley-VCH, New York, 1998.
4 A. Montaser, M. G. Minnich, H. Liu, A. G. T. Gustavsson and R. F. Browner, in *Inductively Coupled Plasma Mass Spectrometry*, ed. A. Montaser, Wiley-VCH, New York, 1998.
5 S.-H. Nam, J.-S. Lim and A. Montaser, *J. Anal. At. Spectrom.*, 1994, **9**, 1357.
6 H. Liu, A. Montaser, S. P. Dolan and R. S. Schwartz, *J. Anal. At. Spectrom.*, 1996, **11**, 307.
7 H. Liu and A. Montaser, *Anal. Chem.*, 1994, **66**, 3233.
8 H. Liu, R. H. Clifford, S. P. Dolan and A. Montaser, *Spectrochim. Acta, Part B*, 1996, **51**, 27.
9 J. W. Olesik, J. A. Kinzer and B. Harkleroad, *Anal. Chem.*, 1994, **66**, 2022.
10 S. A. Pergantis, E. M. Heithmar and T. A. Hinners, *Anal. Chem.*, 1995, **67**, 4530.
11 F. Vanhaecke, M. Van Holderbeke, L. Moens and R. Dams, *J. Anal. At. Spectrom.*, 1996, **11**, 543.
12 S. Augagneur, B. Medina, J. Szpunar and R. Lobinski, *J. Anal. At. Spectrom.*, 1996, **11**, 713.
13 J. S. Becker, H.-J. Dietze, J. A. McLean and A. Montaser, *Anal. Chem.*, 1999, **71**, 3077.
14 D. R. Wiederin, F. G. Smith and R. S. Houk, *Anal. Chem.*, 1991, **63**, 219.
15 M. J. Powell, D. W. Boomer and D. R. Wiederin, *Anal. Chem.*, 1995, **67**, 2474.
16 G. Zoorob, M. Tomlinson, J. Wang and J. Caruso, *J. Anal. At. Spectrom.*, 1995, **10**, 853.
17 S. C. K. Shum and R. S. Houk, *Anal. Chem.*, 1993, **65**, 2972.
18 J. A. McLean, H. Zhang and A. Montaser, *Anal. Chem.*, 1998, **70**, 1012.
19 J. A. McLean, M. G. Minnich, H. Liu, L. A. Iacone and A. Montaser, *J. Anal. At. Spectrom.*, 1998, **13**, 829.
20 B. W. Acon, J. A. McLean and A. Montaser, *Anal. Chem.*, 2000, **72**, 1885.
21 A. Montaser, J. A. McLean and J. M. Kacsir, 1997 US Patent No. 6,166,379, December 26, 2000.
22 B. W. Acon, J. A. McLean and A. Montaser, *J. Anal. At. Spectrom.*, 2001, **16**, 852.
23 J.-L. Todoli and J.-M. Mermet, *J. Anal. At. Spectrom.*, 2001, **16**, 514.
24 S. E. O'Brien, J. A. McLean, B. W. Acon, B. J. Eshelman, W. F. Bauer and A. Montaser, *Appl. Spectrosc.*, 2002, **56**, 1006.
25 K. Kahen, A. Strubinger, J. R. Chirinos and A. Montaser, *Spectrochim. Acta, Part B*, 2003, **58**, 397.
26 S. E. O'Brien, B. W. Acon, S. F. Boulyga, J. S. Becker, H.-J. Dietze and A. Montaser, *J. Anal. At. Spectrom.*, 2003, **18**, 230.
27 H. S. Tan, US Patent # 5,884,846, March 23, 1999.
28 M. E. Ketterer and D. D. Hudson, *J. Anal. At. Spectrom.*, 2000, **12**, 1574.
29 S. E. Hobbs and J. W. Olesik, *Anal. Chem.*, 1992, **64**, 274.
30 M. P. Dziewatkoski, L. B. Daniels and J. W. Olesik, *Anal. Chem.*, 1996, **68**, 1101.
31 J. W. Olesik and C. L. Bates, *Spectrochim. Acta, Part B*, 1995, **50**, 285.
32 R. H. Clifford, P. Sohal, H. Liu and A. Montaser, *Spectrochim. Acta, Part B*, 1992, **47**, 1107.
33 A. Canals, V. Hernandis and R. F. Browner, *Spectrochim. Acta*, 1990, **45B**, 591.
34 J.-L. Todoli, M. Munoz, M. Valiente, V. Hernandis and A. Canals, *Appl. Spectrosc.*, 1994, **48**, 573.
35 D. E. Nixon, *Spectrochim. Acta*, 1993, **48B**, 447.
36 A. Canals, V. Hernandis and R. F. Browner, *J. Anal. At. Spectrom.*, 1990, **5**, 61.
37 J.-L. Todoli, A. Canals and V. Hernandis, *Spectrochim. Acta*, 1993, **48B**, 373.
38 G. Horlick and A. Montaser, in *Inductively Coupled Plasma Mass Spectrometry*, ed. A. Montaser, Wiley-VCH, New York, 1998.
39 A. Gustavsson, *Spectrochim. Acta, Part B*, 1984, **39**, 743.
40 F. J. M. J. Maessen, P. Coevert and J. Balke, *Anal. Chem.*, 1984, **56**, 899.
41 G. Horlick and Y. Shao, *Appl. Spectrosc.*, 1991, **45**, 143.
42 H. Vanhoe, J. Goossens, L. Moens and R. Dams, *J. Anal. At. Spectrom.*, 1994, **9**, 177.
43 R. Tsukahara and M. Kubota, *Spectrochim. Acta, Part B*, 1990, **45**, 581.
44 J. W. Lam and J. W. McLaren, *J. Anal. At. Spectrom.*, 1990, **5**, 419.
45 D. R. Wiederin, R. S. Houk, R. K. Winge and A. P. D'Silva, *Anal. Chem.*, 1990, **62**, 1155.
46 A. Montaser, H. Tan, I. Ishii, S.-H. Nam and M. Cai, *Anal. Chem.*, 1991, **63**, 2660.
47 H. Tao and A. Miyazaki, *J. Anal. At. Spectrom.*, 1995, **10**, 1.
48 M. A. Vaughan and G. Horlick, *Appl. Spectrosc.*, 1986, **40**, 434.